

# The $^{15}\text{N}$ -enrichment in dark clouds and Solar System objects

Hily-Blant P., Bonal L., Faure A., Quirico E.

*Université Joseph Fourier/CNRS, Institut de Planétologie et d'Astrophysique de Grenoble, France*

---

## Abstract

The line intensities of the fundamental rotational transitions of  $\text{H}^{13}\text{CN}$  and  $\text{HC}^{15}\text{N}$  were observed towards two prestellar cores, L183 and L1544, and lead to molecular isotopic ratios  $140 \leq ^{14}\text{N}/^{15}\text{N} \leq 250$  and  $140 \leq ^{14}\text{N}/^{15}\text{N} \leq 360$ , respectively. The range of values reflect genuine spatial variations within the cores. A comprehensive analysis of the available measurements of the nitrogen isotopic ratio in prestellar cores show that molecules carrying the nitrile functional group appear to be systematically  $^{15}\text{N}$ -enriched compared to those carrying the amine functional group. A chemical origin for the differential  $^{15}\text{N}$ -enhancement between nitrile- and amine-bearing interstellar molecules is proposed. This sheds new light on several observations of Solar System objects: *(i)* the similar N isotopic fractionation in Jupiter's  $\text{NH}_3$  and solar wind  $\text{N}^+$ ; *(ii)* the  $^{15}\text{N}$ -enrichments in cometary HCN and CN (that might represent a direct interstellar inheritance); and *(iii)*  $^{15}\text{N}$ -enrichments observed in organics in primitive cosmomaterials. The large variations in the isotopic composition of N-bearing molecules in Solar System objects might then simply reflect the different interstellar N reservoirs from which they are originating.

**Keywords:** astrochemistry, cosmochemistry, Solar Nebula, meteorites, Origin Solar System, radio observations, prestellar cores, objects: L1544, L183

---

## 1. Introduction

Nitrogen, the fifth most abundant element in the Universe, exists naturally as a highly volatile gas ( $\text{N}_2$ , N) and a mixture of compounds of varying volatility (such as  $\text{NH}_3$ , HCN, HNC, *etc.*). The relative abundances and isotopic compositions of these different nitrogen occurrences in various astronomical sources can provide useful clues to the origin and history of the Solar System.

The Sun formed from a cold and dense core embedded in its parental interstellar

molecular cloud rich in gas and dust. The so-called “protosolar nebula” (PSN) is the evolutionary stage issued from the collapsing prestellar core. The nitrogen volatile isotopologues in this nebula may have been fractionated with respect to the original interstellar material, *i.e.* the isotopic ratio measured in these molecules may differ from the elemental ratio. Such fractionation processes are invoked to explain the large enhancements of the D/H ratio measured in several molecular species in prestellar cores (*e.g.* Caselli et al., 2003; Roueff et al., 2005). The efficiency of these

processes however depends on the physical conditions in the core during its collapse (Flower et al., 2006). One of the current challenges in astrochemistry is to follow the chemical composition of a starless core during its evolution towards a planetary system. The related challenge in cosmochemistry is to identify, in primitive objects of the Solar System, residual materials from the original cloud.

The Sun is the largest reservoir of nitrogen in the Solar System. Isotopic measurements of solar wind trapped in lunar soils (Hashizume et al., 2000), analysis of Jupiter’s atmosphere (Fouchet et al., 2000; Owen et al., 2001) and osbornite (TiN), considered as the first solid N-bearing phase to form in the cooling protosolar nebula (Meibom et al., 2007), all independently showed that nitrogen in the PSN was much poorer in  $^{15}\text{N}$  than the terrestrial atmosphere. The analysis of the present-day solar wind trapped on Genesis targets finally concluded on and confirmed these previous studies. The solar wind is depleted in  $^{15}\text{N}$  relative to inner planets and meteorites, and define the following atomic composition for the present-day Sun  $^{14}\text{N}/^{15}\text{N} = 441 \pm 5$  (Marty et al., 2010, 2011). The isotopic composition of nitrogen in the outer convective zone of the Sun has not changed through time and is considered as representative of the PSN. In the present paper, we only consider the original/primary N isotopic fractionation, as opposed to secondary  $^{15}\text{N}$ -enrichments acquired through atmospheric process (*e.g.* Titan, Mars) for example. In the remainder of the paper and for the sake of clarity, the elemental isotopic ratio is noted  $^{14}\text{N}/^{15}\text{N}$ , whilst the isotopic ratio  $X^{15}\text{N}/X^{14}\text{N}$  measured in any N-bearing species X is noted  $\mathcal{R}_X$ .

In our Solar System, any object (with

the exception of Jupiter) is actually enriched in  $^{15}\text{N}$  compared to the PSN (see Fig. 1). Large excesses in  $^{15}\text{N}$  have been found in organic material of chondrites and interplanetary dust particles (IDPs). Enrichments in  $^{15}\text{N}$  are measured at different scales of the material (bulk *vs* hotspots) and can be as high as  $\mathcal{R} = 50$  (Messenger, 2000; Bonal et al., 2010). Molecules in cometary coma also appear to be  $^{15}\text{N}$ -enriched, with  $\mathcal{R}$  ratios varying between 139 and 205 in HCN and CN (see the review by Jehin et al., 2009).

The variation of the nitrogen isotopic composition in Solar System objects is most likely caused by a variety of effects. These include : *(i)* nucleosynthetic origin (Audouze, 1985; Adande and Ziurys, 2012, and references therein); *(ii)* photochemical self-shielding in the solar nebula (Clayton, 2002; Lyons et al., 2009); *(iii)* spallation reactions caused by the irradiation of the young sun (Kung and Clayton, 1978; Chaussidon and Gounelle, 2006); *(iv)* low temperature isotope exchanges (Terzieva and Herbst, 2000, hereafter TH00). The absence of large  $^{15}\text{N}$ -enrichments accross the Galaxy (Adande and Ziurys, 2012, and references therein) and the small fractionation effects predicted by standard gas-phase chemical models (TH00) have weakened so far the hypothesis of a preserved (low temperature) interstellar chemistry to explain the  $^{15}\text{N}$ -enrichments observed in primitive solar cosmomaterials. However, the gas-grain chemical model of Charnley and Rodgers (2002) is able to reach a significant  $^{15}\text{N}$  enrichment of ammonia which is eventually locked into ices. The absence of a direct correlation between D and  $^{15}\text{N}$ -enrichments in organics from primitive cosmomaterials has also been interpreted as the

lack of remnant interstellar chemistry for N isotopologues (Briani et al., 2009; Marty et al., 2010; Aléon, 2010).

In the present work, we analyze the line intensities of the fundamental rotational transitions of  $\text{H}^{13}\text{C}^{14}\text{N}$  and  $\text{H}^{12}\text{C}^{15}\text{N}$  ( $\text{H}^{13}\text{CN}$  and  $\text{HC}^{15}\text{N}$  in the following) towards two starless dense cores, L1544 and L183 (Hily-Blant et al., 2010). The main novelty in our analysis stems from the recent availability of accurate collisional hyperfine selective rate coefficients for HCN with  $\text{H}_2$  (Ben Abdallah et al., 2012). The present work *(i)* brings new observational constraints on nitrogen isotopic fractionation in gas phase and *(ii)* puts a new perspective on the actively debated and long questioning issue of the origin of the  $^{15}\text{N}$ -enrichments observed in primitive cosmo-materials as compared to the protosolar nebula.

## 2. Material and methods

### 2.1. Observations

Observations of the pure rotational  $J = 1 - 0$  lines of  $\text{H}^{13}\text{CN}$  and  $\text{HC}^{15}\text{N}$  were carried out with the IRAM-30m telescope by Hily-Blant et al. (2010). Spectra along perpendicular directions towards the L183 and L1544 starless cores were obtained, with extremely high spectral resolution ( $\nu_0/\delta\nu \approx 4 \times 10^6$ ), such that the hyperfine structure of the  $\text{H}^{13}\text{CN}(1-0)$  is resolved. The details of the observational setup and hardware performances are available in Hily-Blant et al. (2010). The  $\text{H}^{13}\text{CN}$  and  $\text{HC}^{15}\text{N}(1-0)$  spectra towards L183 and L1544 are shown in Fig. A.4. The data are analyzed following a more robust method than the one previously adopted, where column densities were derived under the Local Thermal Equilibrium (LTE) assumption at a temperature

of 8 K. In the present analysis, we make use of the hyperfine structure of the  $\text{H}^{13}\text{CN}(1-0)$  line and of new collisional coefficients for  $\text{HCN-H}_2$  (Ben Abdallah et al., 2012) which were also adopted for  $\text{H}^{13}\text{CN}$  and  $\text{HC}^{15}\text{N}$ .

### 2.2. Data analysis

The analysis of the data makes use of the hyperfine structure of  $\text{H}^{13}\text{CN}$ . The total opacity and excitation temperature of the  $\text{H}^{13}\text{CN}(1-0)$  transition are derived, assuming equal excitation temperature within the hyperfine multiplet. This assumption is justified as long as the opacity remains of the order of unity, which as will be seen later, holds for the lines towards L1544 and L183. The opacity and excitation temperature may then be used to derive the column densities under the LTE assumption (see details in the Appendix). Alternatively, the opacity and line intensity may serve to compute the column density,  $\text{H}_2$  number density, and kinetic temperature, from non-LTE calculations, under the so-called Large Velocity Gradient framework. In such case, we have used the RADEX public code (van der Tak et al., 2007). In these calculations, the  $\text{H}^{13}\text{CN}$  column density is searched for by varying the  $\text{H}_2$  density and the kinetic temperature in the range  $10^{11}$  to  $10^{14} \text{ cm}^{-2}$ ,  $10^3$  to  $10^7 \text{ cm}^{-3}$ , and 5 to 15 K, respectively.

In the case of L183, three methods have been compared. 1/ The HFS method from the CLASS software was applied (see Appendix) with the opacity and the excitation temperature as outputs, which in turn serve to compute a LTE column density. 2/ Another fitting method was based on three independent Gaussians, yet constrained to have the same linewidth, whose peak intensities were used to derive the opacity and the excitation temperature. These two out-

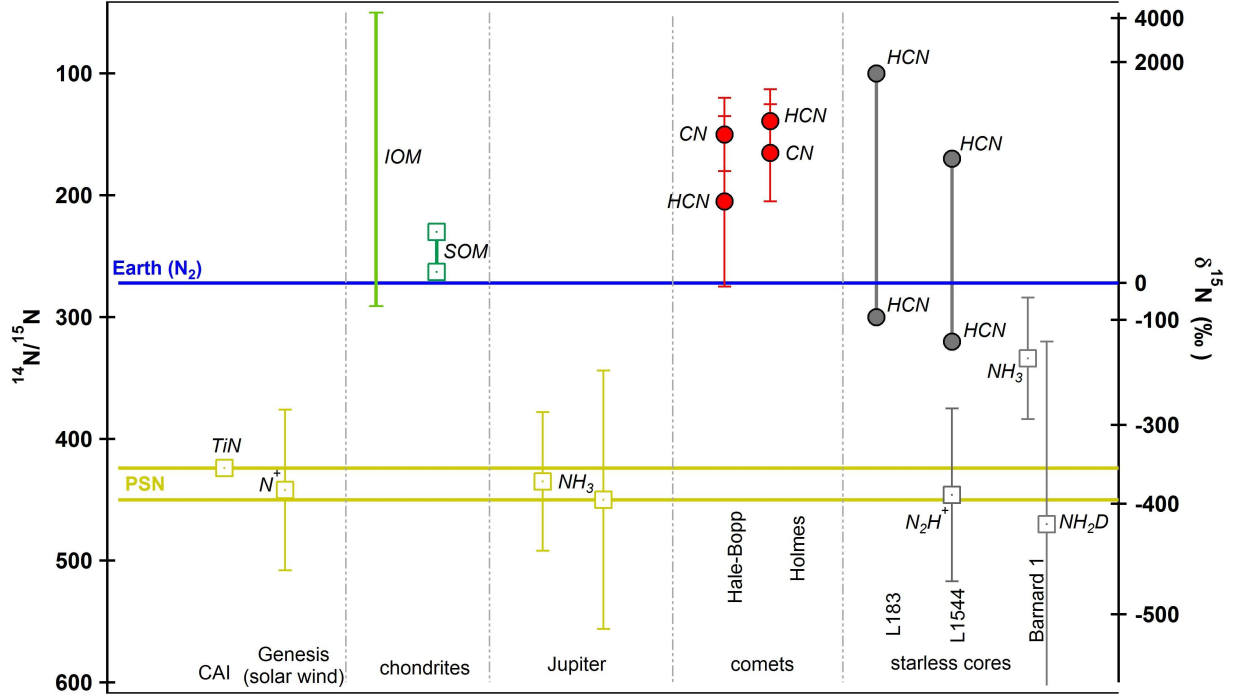


Figure 1: Nitrogen isotopic composition of Solar System objects as compared to the composition of simple molecules in interstellar clouds. The isotopic composition is expressed in term of  $^{14}\text{N}/^{15}\text{N}$  ratios (left scale) and in  $\delta^{15}\text{N}$  notation (right scale,  $\delta^{15}\text{N} = [\mathcal{R}_{\oplus}/\mathcal{R} - 1] \times 1000$ , where  $\mathcal{R}_{\oplus} = 272$  is the nitrogen isotopic composition of the terrestrial atmosphere, see also Table 3). Square and circle symbols are for measurements made on molecules with amine and nitrile functional groups, respectively. IOM stands for Insoluble Organic Matter, SOM for Soluble Organic Matter, and CAI for Calcium-, Aluminum-rich Inclusions. The range of values reported towards L183 and L1544 reflect the spatial variations across the sources.

Table 1: Column densities ( $\times 10^{12} \text{ cm}^{-2}$ ) of  $\text{H}^{13}\text{CN}(1-0)$  from three methods, and of  $\text{HC}^{15}\text{N}$  (LVG calculation) towards L183.

(1)	(2)	(3)	(4)	(5)	(6)	(7)	(8)	(9)	(10)	(11)	(12)	(13)
Offset arcsec	FWHM $\text{km s}^{-1}$	$\tau_0$	$T_{\text{ex}}$ K	$N_{13}$ $\text{cm}^{-2}$	$\tau_0$	$T_{\text{ex}}$ K	$N_{13}$ $\text{cm}^{-2}$	$N_{13}$ $\text{cm}^{-2}$	$N_{15}$ $\text{cm}^{-2}$	$\frac{N_{13}}{N_{15}}$	$\mathcal{R}_{\text{HCN}}$	$\delta^{15}\text{N}$
-40 0	0.36	2.3	2.9	1.8	3.1	2.8	2.3	2.3	—			
-20 0	0.42	1.6	3.2	1.7	1.8	3.0	1.7	1.7	—			
0 -40	0.34	3.7	3.0	2.9	3.4	2.9	2.5	2.7	—			
0 -20	0.33	3.2	3.1	2.5	3.1	2.9	2.2	2.6	0.9	3.1	208	306
0 0	0.47	4.4	3.0	4.7	4.5	2.8	4.4	4.7	1.3	3.7	252	79
0 20	0.42	3.7	3.0	3.5	3.1	2.9	2.8	3.3	1.1	2.9	197	382
0 40	0.36	3.5	3.1	3.0	2.6	2.9	2.0	2.3	1.1	2.0	136	995
20 0	0.43	1.7	3.1	1.7	0.5	3.2	0.5	0.5	—			
40 0	0.46	0.3	3.8	0.4	0.8	3.0	0.8	0.9	—			

**Notes:**

(1): spatial offsets with respect to  $(\alpha, \delta)_{J2000} = (15^{\text{h}}54^{\text{m}}08.80^{\text{s}}, -02^{\circ}52'44.0'')$ .

(2): line width (assumed identical for the three components) from 3-components Gaussian fits, for the 3 hyperfine components.

(3), (4), (5): total center line opacity, excitation temperature, and total  $\text{H}^{13}\text{CN}$  column density ( $10^{12} \text{ cm}^{-2}$ ) in LTE as deduced from a HFS fit in CLASS (see text).

(6), (7), (8): same as above but as derived from the 3-components Gaussian fits.

(9): the column density is calculated in the LVG approximation, from a  $\chi^2$ -minimization against the opacity  $\tau_0$  and the line intensity of the strongest hyperfine component. The column densities only weakly vary with the kinetic temperature in the range 5 to 10 K. The values here correspond to  $T_{\text{kin}} = 8 \text{ K}$ .

(10): column density of  $\text{HC}^{15}\text{N}$  calculated under the LVG approximation for the density and kinetic temperature corresponding to the best solution from the  $\text{H}^{13}\text{CN}$  LVG calculations.

(11), (12), (13): column density ratios and isotopic ratios assuming  $\text{HCN}/\text{H}^{13}\text{CN}=68$ .  $\delta^{15}\text{N} = [\mathcal{R}_{\oplus}/\mathcal{R} - 1] \times 1000$ , where  $\mathcal{R}_{\oplus} = 272$  is the nitrogen isotopic composition of the terrestrial atmosphere

Table 2: Column densities ( $\times 10^{12} \text{ cm}^{-2}$ ) of  $\text{H}^{13}\text{CN}$  and  $\text{HC}^{15}\text{N}$  towards L1544.

(1)	(2)	(3)	(4)	(5)	(6)	(7)	(8)	(9)	(10)
Offset	FWHM	$\tau_i$	$T_{\text{ex}}$	$n_{\text{H}_2}$	$N_{13}$	$N_{15}$	$\frac{N_{13}}{N_{15}}$	$\mathcal{R}_{\text{HCN}}$	$\delta^{15}\text{N}$
arcsec	$\text{km s}^{-1}$		K	$10^4 \text{ cm}^{-3}$	$\text{cm}^{-2}$	$\text{cm}^{-2}$			
-40 40	0.53	2.50	3.1	6.3	5.3	1.7	3.2	215	266
-20 -20	0.40	1.28	3.3	12.5	2.5	0.6	4.5	309	-119
-20 20	0.59	1.86	3.2	10.0	4.7	1.1	4.4	296	-81
0 0	0.46	1.83	3.5	12.5	4.6	1.2	3.8	257	58
20 -20	0.41	2.16	3.3	10.0	4.1	1.2	3.5	238	142
20 20	0.42	1.52	3.1	10.0	2.6	0.9	3.0	207	316
40 -40	0.30	1.68	3.2	10.0	2.4	1.2	2.0	136	993

**Notes:**

(1): spatial offsets with respect to  $(\alpha, \delta)_{J2000} = 05^h 04^m 16.90^s, 25^\circ 10' 47''$ .

(2): line width (assumed identical for the three hyperfine components) from independent Gaussian fits.

(3), (4):  $\text{H}^{13}\text{CN}(1-0)$  center line opacity of the hyperfine component with relative intensity  $\text{RI}=0.5556$ , and excitation temperature, derived from the relative integrated intensities of the three hyperfine components, assuming equal  $T_{\text{ex}}$  for the three hyperfine components.

(5), (6), (7):  $\text{H}_2$  density and total  $\text{H}^{13}\text{CN}$  and  $\text{HC}^{15}\text{N}$  column densities, derived through  $\chi^2$ -minimization accross LVG calculations. Minimization is done in the  $n_{\text{H}_2}, T_{\text{kin}}$  plane using the  $\text{H}^{13}\text{CN}$  opacity and line intensity of the  $\text{RI}=0.5556$  component as constraints. The column density of  $\text{HC}^{15}\text{N}$  derives from LVG calculations at the  $n_{\text{H}_2}, T_{\text{kin}}$  given by  $\text{H}^{13}\text{CN}$ . The values here correspond to  $T_{\text{kin}} = 8 \text{ K}$ .

(8), (9), (10): column density ratios and isotopic ratios assuming  $\text{HCN}/\text{H}^{13}\text{CN}=68$ .

puts give another LTE estimate of the total column density. 3) The opacity and line intensity of a given hyperfine component (*e.g.* the one with  $RI=0.5556$ ) from the latter fitting method were used to derive the column density from LVG calculations. The results of these three methods are summarized in Table 1.

The case of L1544 was tackled in a slightly different fashion, to handle the double peak line profiles, which likely result from two different velocity components along the line of sight rather than infall, as these double peaks are seen in both optically thin and thick tracers. Each hyperfine component was thus fitted as two independent Gaussian profiles, from which an integrated intensity and equivalent linewidth are derived. The relative integrated intensities are used to estimate the opacity and excitation temperature (see Eq. A.2). Finally, the opacity and integrated intensity are  $\chi^2$ -minimized in the  $\{n_{H_2}, N(H^{13}CN)\}$  plane through LVG calculations, at various kinetic temperatures.

The  $HC^{15}N$  column density was obtained from LVG calculations using the  $HC^{15}N(1-0)$  line intensity as a constraint. Solutions in terms of the  $HC^{15}N$  column density are thus obtained by matching the LVG predictions to the observed intensities. Because the hyperfine structure of  $HC^{15}N$  is not resolved out, we adopted the physical conditions derived from the LVG  $H^{13}CN$  analysis while varying only the  $HC^{15}N$  column density. This assumes that the two molecules coexist spatially, which is a reasonable assumption based on simple chemical considerations which show that both molecules derive from the same chemical paths (*e.g.* TH00, Hily-Blant et al., 2010). The signal-to-noise ratio of the  $HC^{15}N$  spectra towards L183 was found to be good enough for only

4 positions. The results of these calculations are given in Tables 1 and 2. The corresponding isotopic ratios are shown in Fig. 2. The typical statistical uncertainty on the derived column densities is 10%. Towards L183, the comparison of the column density resulting from the three methods provide a more reliable estimate of the uncertainty on the column density determination, of the order of 20%. Towards L1544, we have used separately the  $RI=0.3333$  and  $RI=0.5556$  line intensities as constraints, which results in a dispersion of 10 to 30%.

### 2.3. Results

The excitation temperatures are in the range 3–4 K, which is significantly lower than the value assumed by Hily-Blant et al. (2010), but very close to the values determined by Padovani et al. (2011) towards other starless cores. The associated column densities lead to isotopic ratios  $H^{13}CN/HC^{15}N = 2$  to 4.5. As is evident from Fig. 2, the LVG column densities of both  $H^{13}CN$  and  $HC^{15}N$  depend only slightly on the kinetic temperature. Within a given source, the range of values for the isotopic ratio reflects genuine spatial variations across the source. These variations are up to a factor of 2 in L1544.

To derive the isotopic ratio  $\mathcal{R}_{HCN}$  we assumed that  $[HCN]/[H^{13}CN] = [^{12}C]/[^{13}C]$ , such that

$$\frac{[HCN]}{[HC^{15}N]} = \frac{[H^{13}CN]}{[HC^{15}N]} \times \frac{[^{12}C]}{[^{13}C]}. \quad (1)$$

This amounts in assuming that HCN does not undergo significant carbon fractionation and that the  $HCN/H^{13}CN$  ratio reflects the elemental ratio. Carbon fraction of HCN is unlikely for several reasons. First, most of the carbon is locked into CO and  $^{13}CO$ , and little carbon ions are then available for

isotope exchange. In addition, Milam et al. (2005) concluded that CN is at most only weakly affected by chemical fractionation, and the chemical similarity between CN and HCN led Adande and Ziurys (2012) to argue that carbon fractionation of HCN must be small. Last, it is to be noted that chemical fractionation would increase the  $\text{H}^{13}\text{CN}/\text{HCN}$  hence driving the molecular isotopic ratio  $\mathcal{R}_{\text{HCN}}$  towards lower values. We thus argue that the nitrogen fractionation observed in HCN is robust. For the elemental isotopic ratio  $^{12}\text{C}/^{13}\text{C}$  of carbon, we adopt the value of 68 from Milam et al. (2005). The values for this ratio range from 140 to 360 towards L1544, and from 140 to 250 towards L183. These values are significantly lower than the isotopic ratios reported by Bizzocchi et al. (2010) towards L1544, using  $\text{N}_2\text{H}^+$  as a tracer. They are also well below the ratios determined towards other cores by Gerin et al. (2009) and Lis et al. (2010), who used  $\text{NH}_2\text{D}$  and  $\text{NH}_3$  as nitrogen carriers, respectively (see Fig. 1). In contrast, these values encompass the low ratio  $\mathcal{R}_{\text{HCN}} = 150$  determined by Ikeda et al. (2002) towards L1521E.

In the following, we compare these results with isotopic ratios in Solar System objects, and propose a unified view of these measurements based on simple chemical arguments.

### 3. Discussion

#### 3.1. Differential fractionation for nitriles and amines

In prestellar cores, millimeter observations show that in contrast to CO, nitrogen-bearing species such as CN and HCN manage to remain in appreciable amounts in the gas phase (Hily-Blant et al., 2008; Padovani et al., 2011). In such environments, isotope exchange reactions are the

only source of fractionation. These are caused by a thermodynamic effect in which the exchange of isotopic atoms within a reaction has a preferred direction owing to exothermicity, which is caused by zero point energy differences. This process is efficient when the temperature is lower than the exothermicity, provided that the exchange reactions are competitive with other reactions. Rodgers and Charnley (2008) have shown theoretically that significant  $^{15}\text{N}$  enhancements can occur for various molecules in N-rich prestellar cores depleted in CO and OH. As recognized by these authors, however, their chemical model is hampered by the lack of accurate rate coefficients for the numerous isotopologue exchange reactions, which drive the fractionation.

Among the amines detected in prestellar cores,  $\text{NH}_3$  and its deuterated isotopologues, and  $\text{N}_2\text{H}^+$ , present isotopic ratios of the order of 400 or larger (Gerin et al., 2009; Lis et al., 2010; Bizzocchi et al., 2010). In contrast, HCN shows significantly lower values such as  $\mathcal{R}_{\text{HCN}} = 150$  toward L1521E (Ikeda et al., 2002) and 150 – 260 towards L1544 (Milam and Charnley, 2012). These values are all consistent with our new measurements towards L183 and L1544, also based on HCN observations. Put all together, these observations suggest a differential behaviour of nitriles and amines with respect to fractionation (see Fig. 1 and Table 3). This is indeed also visible in the gas-phase model of TH00, though at very low levels, and at a higher level in the gas-grain model of Rodgers and Charnley (2008).

A comprehensive analysis of nitrogen interstellar chemistry in dark clouds is summarized in Fig. 3. It appears that N-bearing molecules can be divided into two almost distinct chemical families: those carrying the nitrile ( $-\text{CN}$ ) functional group and those



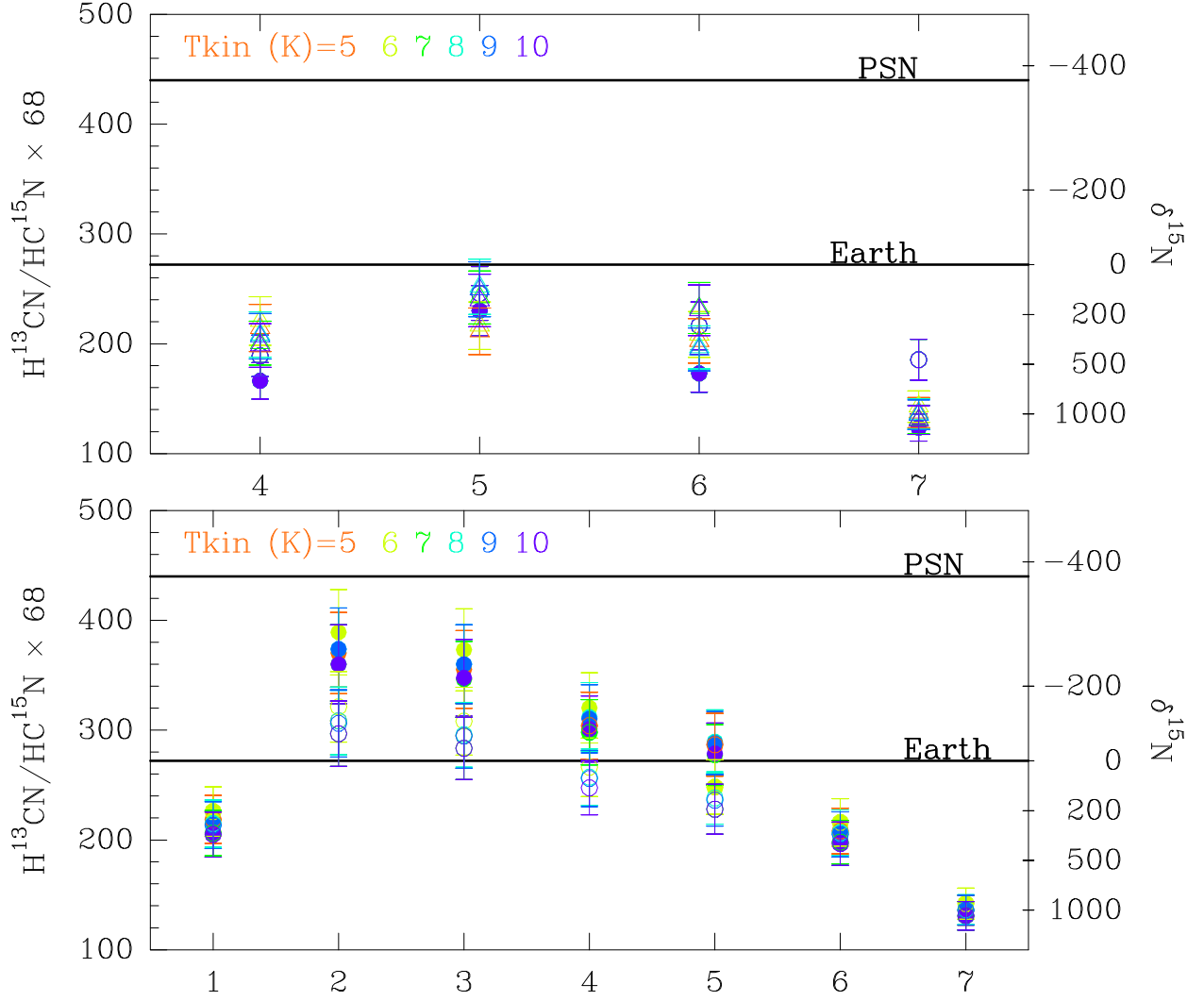


Figure 2: Nitrogen isotopic ratio  $\mathcal{R}_{\text{HCN}}$  as measured towards L183 (upper panel) and L1544 (lower panel). Measurements for several positions are reported for each core (see also Tables 1 and 2). The isotopic enrichment in delta notation is indicated on the right scale. In each panel, the thick lines indicate the protosolar nebula value of  $441 \pm 5$  (Marty et al., 2011) and the terrestrial reference ( $^{14}\text{N}/^{15}\text{N} = 272$ ). The ratios determined for kinetic temperatures ranging from 5 to 10 K are shown. At each position and for each kinetic temperature, several values are displayed, which correspond to different analysis methods (see Appendix for details).

carrying the amine (-NH) functional group. The former family derives from atomic nitrogen while the latter are formed *via*  $N^+$ , which is the product of  $N_2$  dissociative ionization. As a consequence, these two families are not expected to exchange their  $^{15}N$ . On the other hand, the  $^{14}N/^{15}N$  exchange reactions among nitriles and amines most likely present different time scales and/or efficiency (TH00, Rodgers and Charnley, 2008). Different  $^{15}N$  enhancements are therefore expected between *e.g.*  $NH_3$  and HCN, even if rate coefficients are uncertain.

The present work also shows that the nitrogen isotopic ratio varies inside a given prestellar core. Although a variety of physical parameters (density, temperature), known to present spatial variations in these objects, could be invoked to explain these inhomogeneities, source modelling including radiative transfer and chemistry is most likely needed to draw conclusions in this regard. Yet, in the context of this work, these spatial variations may be related with the large range of values measured in the Solar System.

### 3.2. Potential N reservoirs sampled by Solar System objects

Similarly to interstellar clouds, the PSN was most likely composed of several nitrogen reservoirs characterized by different relative abundances and isotopic compositions. In interstellar clouds, molecules carrying the nitrile functional group appear to be systematically  $^{15}N$ -enriched compared to molecules carrying the amine group (see Section 1 and Fig. 1). Thus, we propose that the highly variable  $^{14}N/^{15}N$  ratios in objects of the Solar System might simply reflect the interstellar nitrogen reservoir from which they are originating. The Sun and giant planets, sampled atomic and/or molec-

ular nitrogen, considered as the major reservoir in the PSN. Asteroids and comets, that are N-depleted compared to the Sun, may have sampled minor, less volatile, and isotopically fractionated N reservoirs of compounds such as HCN. These are found to be systematically  $^{15}N$ -enriched compared to the Sun, hence the PSN. In the following paragraphs, we discuss in details each of these issues.

### 3.3. Variable fractionation in Solar System objects

Nitrogen isotopic composition was determined using ammonia in the atmosphere of Jupiter (Fouchet et al., 2000; Owen et al., 2001) leading to  $\mathcal{R}_{NH_3} \approx 440$ . It is now largely interpreted as representative of the average value for nitrogen in the solar nebula. The similarity of the high Jovian and nebular  $\mathcal{R}_{NH_3}$  and  $\mathcal{R}_{N^+}$  ratios, respectively, reinforces the ideas that molecules carrying the amine functional group, deriving from  $N_2$ , are not fractionated.

Comets may have better preserved than asteroids the volatile molecules that were present in the protosolar cloud. The abundances of the simple molecules such as CO,  $CO_2$ ,  $CH_3OH$ ,  $H_2CO$  and HCN suggest indeed the partial preservation of an interstellar component (Irvine et al., 2000). These molecules, present as ices in the nucleus, are detected in the coma after their sublimation when the comets approach the sun. HCN is the most abundant N-bearing molecule that has been detected so far (directly or through the CN radical), and also the only one whose nitrogen isotopic composition was measured. There has been some debate whether the radical CN is produced through the photodissociation of HCN, or is a thermo-degradation product of refractory CHON grains (Fray et al.,

Table 3: Nitrogen isotopic ratios in Solar System objects and in the cold ISM.

Probe	Source	$\mathcal{R}^\dagger$	$\delta^{15}\text{N}^\ddagger$	References
NH <sub>2</sub> D	Barnard 1	$470 \pm 150$	$-420 \pm 180$	Gerin et al. (2009)
	L1689B	$810^{+600}_{-250}$	$[-800 : -500]$	Gerin et al. (2009)
NH <sub>3</sub>	Barnard 1	$334 \pm 50$	$-180 \pm 120$	Lis et al. (2010)
N <sub>2</sub> H <sup>+</sup>	L1544	$446 \pm 71$	$-390 \pm 100$	Bizzocchi et al. (2010)
HCN	L1521E	150	815	Ikeda et al. (2002)
	L183	[140: 250]	[1000: 80]	This work
	L1544	[140: 360]	[1000:-245]	This work
Amino Acids		[263:230]	[37:184]	Sephton et al. (2002)
IOM (bulk)		< 195	400	Alexander et al. (2007)
IOM (hotspots)		< 65	3200	Busemann et al. (2006)
Isheyevo - clasts		50	4450	Bonal et al. (2010)
IDPs (bulk)		[305:180]	[-107: 514]	Floss et al. (2006)
IDPs (hotspots)		up to 118	1300	Floss et al. (2006)

$^\dagger$  Molecular isotopic ratio measured in a given N-bearing species.

$^\ddagger$  Deviation from the standard terrestrial value in parts per thousand defined as  $\delta^{15}\text{N} = [\mathcal{R}_\oplus/\mathcal{R} - 1] \times 1000$ , where  $\mathcal{R}_\oplus = 272$  is the nitrogen isotopic composition of the terrestrial atmosphere.

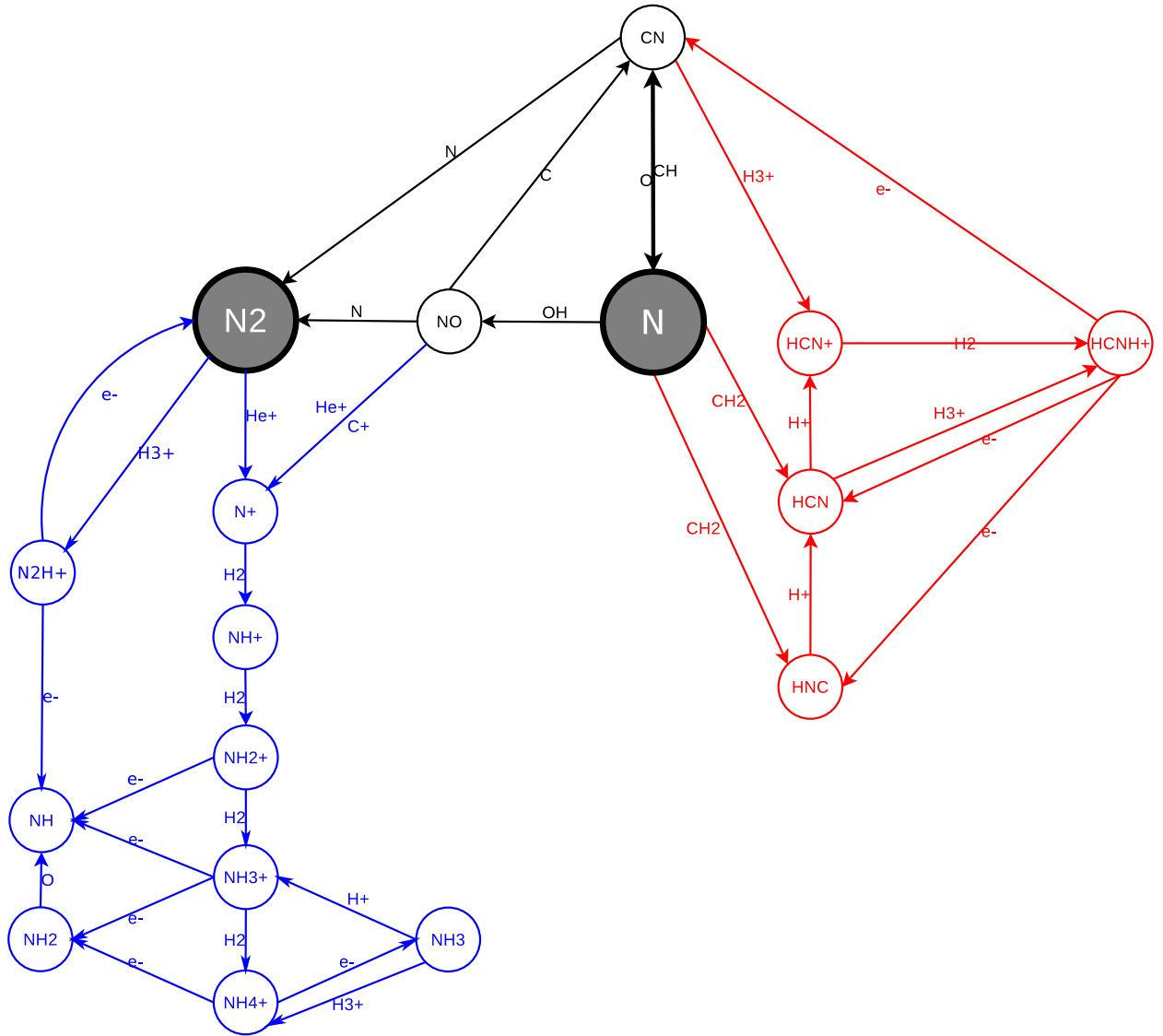


Figure 3: Principal gas-phase reactions involved in the interstellar chemistry of nitrogen in dense clouds where UV photons can be ignored . Amines (left) and nitriles (right) have been clearly separated.

2005). However, a genetic link between HCN and CN is strengthened based in their comparable nitrogen isotopic compositions deduced from a careful data reanalysis (Bockelée-Morvan et al., 2008) and on consistent production rates (Paganini et al., 2010). Therefore, a relevant comparison between cometary molecules and ISM is possible through the same molecular species: HCN. The CN nitrogen isotopic composition was measured in a large number of Oort Cloud comets ( $^{14}\text{N}/^{15}\text{N}_{\text{ave}} = 144 \pm 6.5$ ) and Jupiter family comets, ( $^{14}\text{N}/^{15}\text{N}_{\text{ave}} = 156.8 \pm 12.2$ ) revealing a large and fairly constant nitrogen fractionation ( $130 < ^{14}\text{N}/^{15}\text{N} < 170$ ) with no dependence on the origin and heliocentric distance of the observed comets (see the reviews by Jehin et al., 2009; Manfroid et al., 2009, and references therein). These ratios are similar to the lowest ones in dark clouds L1544 and L183 (see Fig. 1) but do not reflect the spatial heterogeneity seen in these two dark clouds. However, these two clouds do not evidence the same levels of heterogeneity, and one possible explanation might be that the PSN emerged from a more homogeneous dark cloud than L183. In addition, only a small mass fraction of the material from the dark cloud – that may be more homogenous – is eventually incorporated stars and planetary systems. Last, potential isotopic heterogeneity of a cometary nucleus could remain undetected, since observations from the ground generally provide an averaged measurement of the coma (*e.g.* Blake et al., 1999). The N isotopic composition of HCN in comets is therefore consistent with an interstellar heritage. The preservation of cometary ices highly depends on the thermal history of the objects. The actual presence of the highly volatile HCN in comets attests of the absence of sig-

nificant heating. Moreover, only few processes are expected to modify the nitrogen isotopic composition of the HCN molecule after its formation. Indeed, nitrogen atoms are not easily exchangeable unlike protons that easily exchange with ice. Evidences were provided experimentally for protons in methanol (Ratajczak et al., 2009) and through observations in HCN (Blake et al., 1999). In this regard, the  $\mathcal{R}$  ratio may appear as a more reliable proxy of the origin of the molecule than the D/H ratio.

Chondrites might not be considered as a representative sampling of the nitrogen in the PSN. Indeed, asteroids, hence chondrites, most likely did not accrete the highly volatile nitrogen reservoirs ( $\text{N}_2$  and N). Thus, the  $^{15}\text{N}$ -enriched organics in chondrites might have originally sampled some of the minor reservoirs made of nitrogen compounds such as HCN and N-bearing molecules of higher molecular weight.

Carbonaceous chondrites contain up to 5% elemental carbon in a variety of forms, organic matter being the major one. A minor fraction (less than 25%) of the organic matter in carbonaceous chondrites is present as relatively low-molecular-weight compounds, extractable with common organic solvents, the so-called “soluble organic matter” (SOM). SOM consists in a complex mix of organic molecules bearing H, C, O, N, S, and P elements, with masses up to 800 amu (Sephton et al., 2002; Gilmour, 2003; Schmitt-Koplin et al., 2010). The remaining fraction (75% or so) is present as a high-molecular-weight macromolecular material, persisting after harsh demineralization of the chondrites, the so-called “insoluble organic matter” (IOM). Interplanetary Dust Particles (IDPs) and Antarctic micrometeorites (AMMs) are micrometric particles that have either an

asteroidal or a cometary origin. They also contain organics that present similarities with those of carbonaceous chondrites (Dobrică et al., 2011).

The soluble and insoluble organic fractions both contain some nitrogen and are characterized by  $^{15}\text{N}$ -enrichments relatively to the PSN. The nitrogen isotopic compositions of amino acids have mostly been determined in the Murchison chondrite (Pizzarello et al., 1994; Engel and Macko, 1997). The  $\mathcal{R}$  ratios are typically between 230 and 263. The isotopic fractionation is obviously reported on amine functional groups that are not fractionated in our model scheme (see Fig. 3 and Sect. 3.1). The origin of amino acids is yet unknown. Multiple pathways of formation have been proposed in the literature. Some recent experiments on interstellar ices analogs showed that a viable model of formation is based on nitriles as amino acids precursor molecules (Elsila et al., 2007). Hence the nitrogen isotopic composition of amino acids might reflect that of the precursor HCN and not that of  $\text{NH}_3$ .

Nitrogen is a minor element of IOM (2% in weight in average Alexander et al., 2007). It is mostly present in heterocycles such as pyrroles (*e.g.* Sephton et al., 2003; Remusat et al., 2005; Derenne and Robert, 2010). The contribution of N as present in nitriles appears to be relatively low ( $N_{\text{pyrrole}}/N_{\text{nitrile}} = 5$  in Murchison; Derenne and Robert, 2010). The most primitive chondrites are characterized by bulk  $^{15}\text{N}$ -enrichments up to  $\mathcal{R} = 195$  (Alexander et al., 2007). Chondritic clasts in the unique Isheyevo meteorite are characterized by the highest bulk  $^{15}\text{N}$ -enrichment at the present day, with  $\mathcal{R} = 50$  (Bonafant et al., 2010). Analytical techniques

with submicron-scale imaging abilities revealed very localized  $^{15}\text{N}$ -enrichments (commonly referred to as  $^{15}\text{N}$ -hotspots), up to  $\mathcal{R} = 65$  (Busemann et al., 2006). Due to the experimental challenges implied by their micron-scale size, SOM and IOM in IDPs are not isolated; only isotopic compositions of bulk material are measured. High  $^{15}\text{N}$ -enrichments were revealed in IDPs; bulk such as  $180 < \mathcal{R} < 305$  - hotspots up to  $\mathcal{R} = 118$  (Floss et al., 2006). As a summary, similar  $^{15}\text{N}$ -enrichments are measured in bulk IOM of cosmomaterials and in HCN in L1544 and L183. However, to be meaningful the comparison between ISM and cosmomaterials must be based on similar molecules (*e.g.* HCN in comets) or on molecules linked by determined chemical pathways (*e.g.*  $^{15}\text{N}$  of amino acids inherited from nitriles precursors). The chemical carriers of the isotopic anomalies (bulk and hotspots) in the IOM are not identified yet. They may be located onto heterocycles, nitriles, and/or unidentified chemical group or compound. The IOM as currently observed in cosmomaterials was most likely synthesized through multistep processes that possibly involved recycling of interstellar species within the protosolar disk (Sephton et al., 2002; Dartois et al., 2004; Okumura and Mimura, 2011). As a consequence, it is impossible to draw a direct link between the  $^{15}\text{N}$ -enrichments in the IOM of cosmomaterials to interstellar molecules or to a series of chemical reactions as they are expected to occur in ISM. Furthermore, physical processes like radiolysis or heating could have modified IOM or even be involved in its synthesis (*e.g.* Huss et al., 2003). Little is known about the isotopic fractionation due to these processes, a significant role cannot be excluded. Hence a genetic link between ISM molecules and

IOM cannot be currently firmly established, but is at least suggested based on consistent  $^{15}\text{N}$ -enrichments.

#### 4. Conclusions and perspectives

Among the arguments against the idea of interstellar chemistry at the origin of  $^{15}\text{N}$ -enrichments in organics of primitive cosmo-materials are: *(i)* the assumption of nitrogen isotopic ratios of the order of 400 or higher in interstellar HCN and  $\text{NH}_3$ ; *(ii)* the failure of classical gas-phase ion-molecule reactions in interstellar chemical models to produce large  $^{15}\text{N}$ -enrichments TH00; *(iii)* the absence of spatial correlation between D- and  $^{15}\text{N}$ -enrichments in primitive organics is interpreted as a proof of different processes at their origins (Briani et al., 2009; Aléon, 2010; Marty et al., 2010).

The observations reported here irrevocably show that considerable nitrogen isotopic fractionation occurs at low temperature in the gas phase of prestellar cores. These new measurements provide strong constraints to interstellar chemistry models and are consistent with the early-time chemistry predicted by the gas-grain model of Rodgers and Charnley (2008). Moreover, even though fractionation of both hydrogen and nitrogen might reflect low-temperature gas-phase chemistry, it is probably not driven by the same molecular carriers. Indeed, the isotopic composition of a given species is determined by the complex interplay of a reaction network and the isotopic compositions of the precursors. In addition, the typical exothermicities of reactions leading to D-enrichments and  $^{15}\text{N}$ -enrichments are different ( $\approx 230$  K and  $\approx 30$  K, respectively) and leave room for a differential fractionation between hydrogen and nitrogen, depending on the ther-

mal history of prestellar cores. Last, it was recently shown that varying the ortho-to-para ratio of  $\text{H}_2$  in interstellar chemistry can lead to D-enrichments and at the same time inhibit nitrogen fractionation (Wirström et al., 2012). There is thus little reason to expect correlated isotopic anomalies between these two elements.

Even though the link between organics in primitive cosmomaterials and interstellar molecules cannot be directly determined, isotopic fractionation is a strong diagnostic feature. The present study evidences that the large nitrogen fractionations observed in comets and chondrites are consistent with a presolar chemistry. Several arguments used against such an idea are here clearly invalidated.

#### Appendix A. Column density determination

For a resolved hyperfine structure spectrum, such as  $\text{H}^{13}\text{CN}(1-0)$ , the assumption of a common excitation temperature for all hyperfine components allows a derivation of the excitation temperature and of the opacity of each component. Radiative transfer through gas with a constant excitation temperature leads to the following expression for the emergent intensity in ON-OFF observing mode:

$$T_{\text{mb}} = [J_{\nu}(T_{\text{ex}}) - J_{\nu}(2.73)] (1 - e^{-\tau}) = \Delta J_{\nu}(T_{\text{ex}}) (1 - e^{-\tau}) \quad (\text{A.1})$$

with  $J_{\nu}(T) = T_0/[1 - \exp(-T_0/T)]$  and  $T_0 = h\nu/k$ . Noting  $r_k$  the relative intensities of the various components of a hyperfine multiplet, the ratio of the opacities of two components is  $\tau_i/\tau_j = r_i/r_j$ . Hence, assuming a constant  $T_{\text{ex}}$  for all hyperfine components of a given multiplet, one directly

obtains from Eq. A.1, that

$$\frac{T_{\text{mb},i}}{T_{\text{mb},j}} = \frac{1 - \exp(-r_i\tau_0)}{1 - \exp(-r_j\tau_0)} \quad (\text{A.2})$$

where we choose  $\sum_i r_i = 1$  and we have noted  $\tau_0 = \sum_i \tau_i$ . From the measured  $T_{\text{mb}}$  and known  $r_i$ , it is thus possible to derive  $\tau_0$ , from which the excitation temperature follows by inverting Eq. A.1. For lines of moderate opacity ( $\tau_0 < 1$ ), peak or integrated intensity ratios may be used with no difference. The column density is then obtained directly from the integrated opacity of the hyperfine component  $k$  as:

$$N_{\text{tot}} = \frac{8\pi\nu^3}{c^3} \frac{Q(T_{\text{ex}})}{A_k g_k} \frac{\int \tau_k(v) dv}{1 - e^{-T_0/T_{\text{ex}}}} = \mathcal{N}_k(T_{\text{ex}}) \int \tau_k(v) dv \quad (\text{A.3})$$

The HFS method of the CLASS software, used in the case of L183, fits simultaneously the hyperfine components with Gaussians, by fixing their relative positions and intensities. Fit results are shown in Fig. A.4. In the case of L1544, the double-peak nature of the emission spectrum made this procedure unfruitful. The adopted strategy therefore was to first determine the integrated intensity of each hyperfine component as obtained from independent double-Gaussian fit (see Fig. A.5 and A.6). The relative integrated intensities were then used to derive the opacity and excitation temperature through Eq. A.2.

## References

- Adande, G.R., Ziurys, L.M., 2012. Millimeter-wave Observations of CN and HNC and Their  $^{15}\text{N}$  Isotopologues: A New Evaluation of the  $^{14}\text{N}/^{15}\text{N}$  Ratio across the Galaxy. *ApJ* 744, 194.  
Aléon, J., 2010. Multiple Origins of Nitrogen Isotopic Anomalies in Meteorites and Comets. *ApJ* 722, 1342–1351.

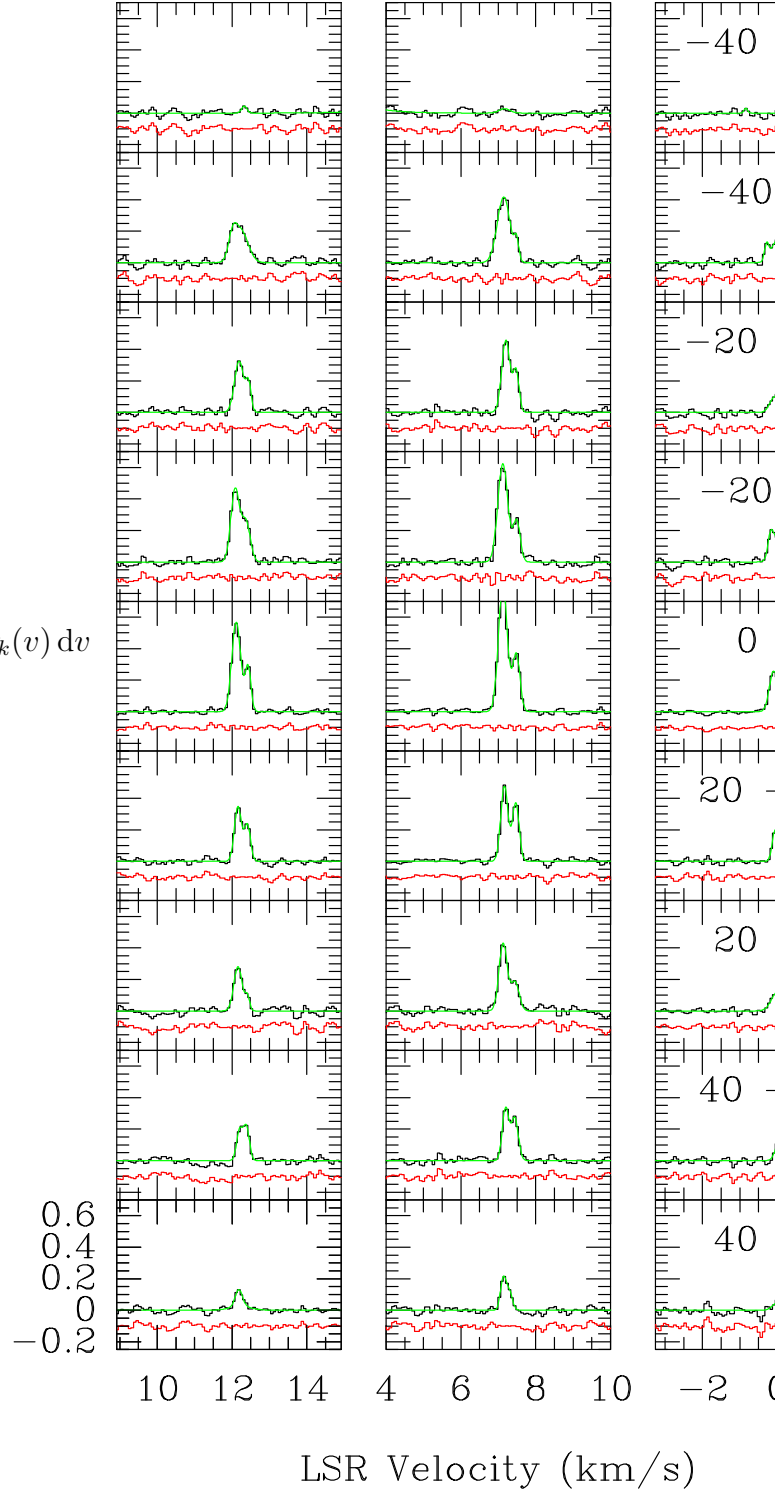


Figure A.5: Results of the Gaussian fitting procedure applied to  $\text{H}^{13}\text{CN}(1-0)$  towards L1544 (see Sect. 2). On each row, the three hyperfine components are shown in separate panels emphasize the double peak profile. The residuals are shown below the original spectrum. The fit result is overlaid on top of the spectrum.



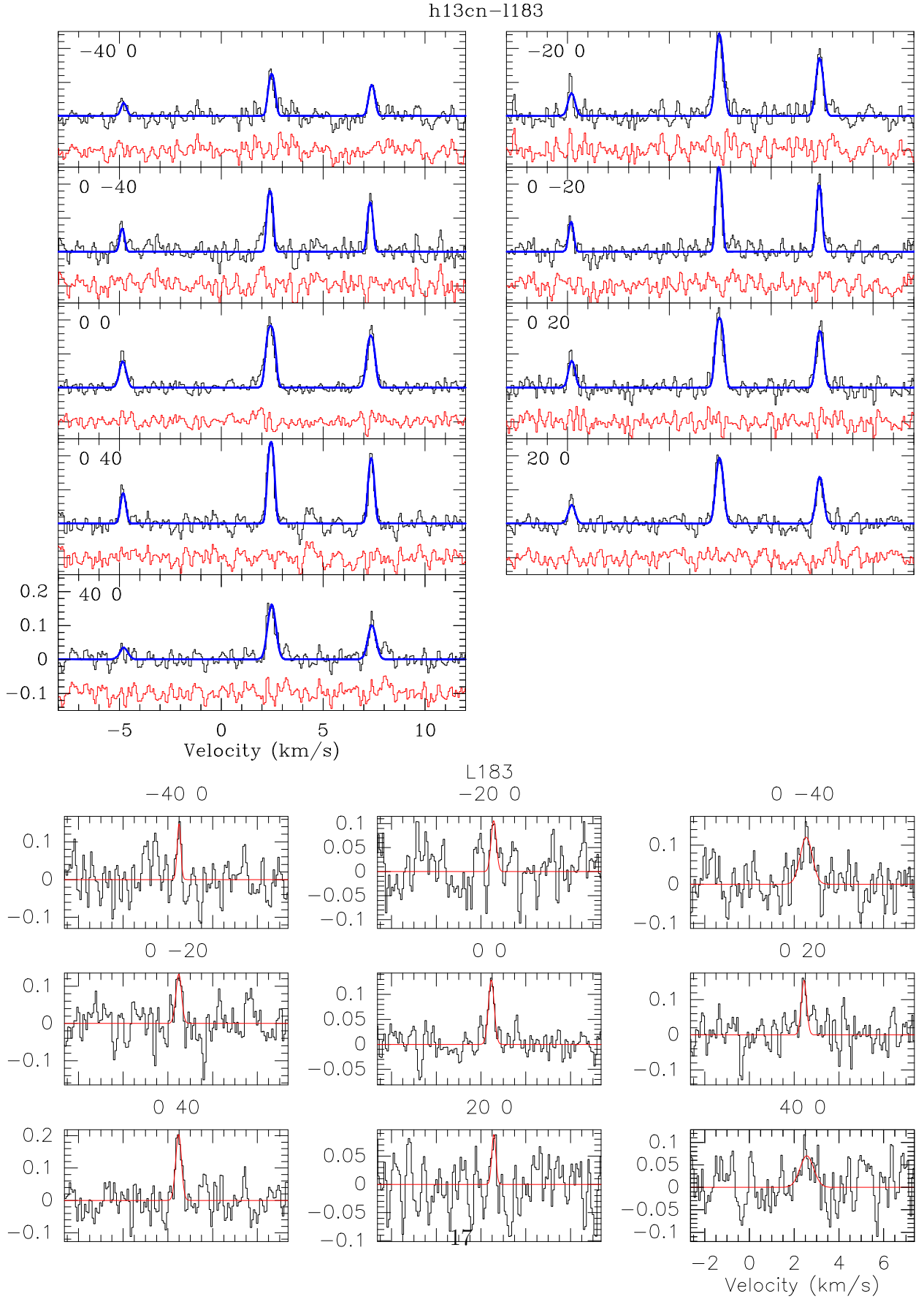


Figure A.4: *Top*: Results of the  $\text{H}^{13}\text{CN}(1-0)$  hyperfine structure fitting procedure towards L183 for each spatial position (offsets in arcsec are indicated). The residuals are shown below the original spectrum. The fit result is overlaid on top of the spectrum. *Bottom*:  $\text{HC}^{15}\text{N}(1-0)$  spectra. Results from single-component Gaussian fits are shown.

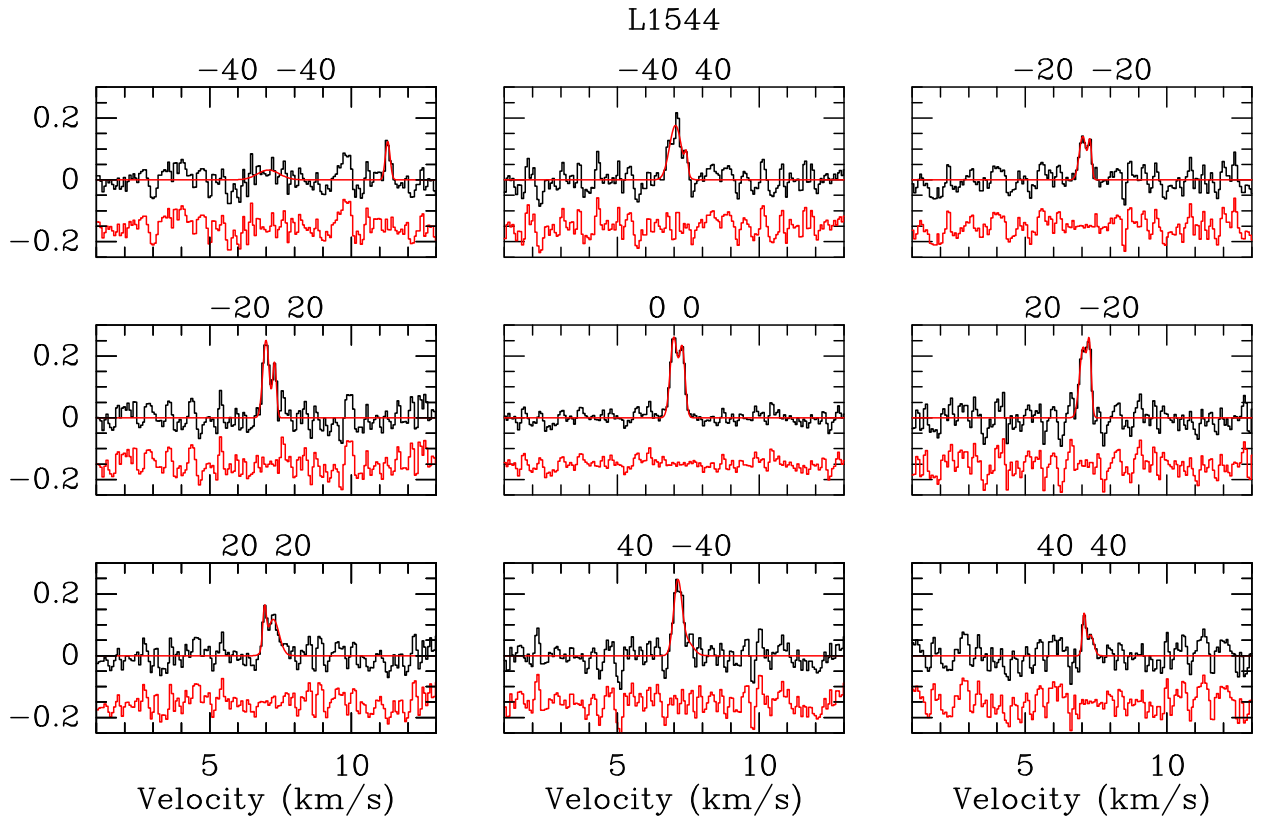


Figure A.6:  $\text{HC}^{15}\text{N}(1-0)$  spectra towards L1544. Gaussian fits are overlaid on top of each spectrum, and the residuals are shown below.

- Alexander, C.M.O., Fogel, M., Yabuta, H., Cody, G.D., 2007. The origin and evolution of chondrites recorded in the elemental and isotopic compositions of their macromolecular organic matter. *Geochim. Cosmochim. Ac.* 71, 4380–4403.
- Audouze, J., 1985. C, N and O isotopes and chemical evolution of our Galaxy, in: I. J. Danziger, F. Matteucci, & K. Kjar (Ed.), *European Southern Observatory Conference and Workshop Proceedings*, pp. 373–384.
- Ben Abdallah, D., Najar, F., Jaidane, N., Dumouchel, F., Lique, F., 2012. Hyperfine excitation of HCN by H<sub>2</sub> at low temperature. *MNRAS* 419, 2441–2447.
- Bizzocchi, L., Caselli, P., Dore, L., 2010. Detection of N<sup>15</sup>NH<sup>+</sup> in L1544. *A&A* 510, L5. 1001.4903.
- Blake, G.A., Qi, C., Hogerheijde, M.R., Gurwell, M.A., Muhleman, D.O., 1999. Sublimation from icy jets as a probe of the interstellar volatile content of comets. *Nature* 398, 213–216.
- Bockelée-Morvan, D., Biver, N., Jehin, E., Cochran, A.L., Wiesemeyer, H., Manfroid, J., Hutsemékers, D., Arpigny, C., Boissier, J., Cochran, W., Colom, P., Crovisier, J., Milutinovic, N., Moreno, R., Prochaska, J.X., Ramirez, I., Schulz, R., Zucconi, J.M., 2008. Large Excess of Heavy Nitrogen in Both Hydrogen Cyanide and Cyanogen from Comet 17P/Holmes. *ApJ* 679, L49–L52. 0804.1192.
- Bonal, L., Huss, G.R., Krot, A.N., Nagashima, K., Ishii, H.A., Bradley, J.P., 2010. Highly <sup>15</sup>N-enriched chondritic clasts in the CB/CH-like meteorite Isheyevo. *Geochim. Cosmochim. Ac.* 74, 6590–6609.
- Briani, G., Gounelle, M., Marrocchi, Y., Mostefaoui, S., Robert, F., Leroux, H., Meibom, A., 2009. Ultra-Pristine Extra-Terrestrial Material with Unprecedented Nitrogen Isotopic Variation, in: *Lunar and Planetary Institute Science Conference Abstracts*, p. 1642.
- Busemann, H., Young, A.F., O’D. Alexander, C.M., Hoppe, P., Mukhopadhyay, S., Nittler, L.R., 2006. Interstellar Chemistry Recorded in Organic Matter from Primitive Meteorites. *Science* 312, 727–730.
- Caselli, P., van der Tak, F.F.S., Ceccarelli, C., Bacmann, A., 2003. Abundant H<sub>2</sub>D<sup>+</sup> in the pre-stellar core L1544. *A&A* 403, L37–L41. [arXiv:astro-ph/0304103](#).
- Charnley, S.B., Rodgers, S.D., 2002. The End of Interstellar Chemistry as the Origin of Nitrogen in Comets and Meteorites. *ApJ* 569, L133–L137.
- Chaussidon, M., Gounelle, M., 2006. *Irradiation Processes in the Early Solar System*. University of Arizona Press, Tucson. pp. 323–339.
- Clayton, R.N., 2002. Solar System: Self-shielding in the solar nebula. *Nature* 415, 860–861.
- Dartois, E., Muñoz Caro, G.M., Deboffle, D., d’Hendecourt, L., 2004. Diffuse interstellar medium organic polymers. Photoproduction of the 3.4, 6.85 and 7.25  $\mu$ m features. *A&A* 423, L33–L36.
- Derenne, S., Robert, F., 2010. Model of molecular structure of the insoluble organic matter isolated from Murchison meteorite. *Meteoritics and Planetary Science* 45, 1461–1475.
- Dobrică, E., Engrand, C., Quirico, E., Montagnac, G., Duprat, J., 2011. Raman characterization of carbonaceous matter in CONCORDIA Antarctic micrometeorites. *Meteoritics and Planetary Science* 46, 1363–1375.
- Elsila, J.E., Dworkin, J.P., Bernstein, M.P., Martin, M.P., Sandford, S.A., 2007. Mechanisms of Amino Acid Formation in Interstellar Ice Analogs. *ApJ* 660, 911–918.
- Engel, M.H., Macko, S.A., 1997. Isotopic evidence for extraterrestrial non-racemic amino acids in the Murchison meteorite. *Nature* 389, 265–268.
- Floss, C., Stadermann, F.J., Bradley, J.P., Dai, Z.R., Bajt, S., Graham, G., Lea, A.S., 2006. Identification of isotopically primitive interplanetary dust particles: A NanoSIMS isotopic imaging study. *Geochim. Cosmochim. Ac.* 70, 2371–2399.
- Flower, D.R., Pineau des Forêts, G., Walmsley, C.M., 2006. The importance of the ortho:para H<sub>2</sub> ratio for the deuteration of molecules during pre-protostellar collapse. *A&A* 449, 621–629. [arXiv:astro-ph/0601429](#).
- Fouchet, T., Lellouch, E., Bézard, B., Encrenaz, T., Drossart, P., Feuchtgruber, H., de Graauw, T., 2000. ISO-SWS Observations of Jupiter: Measurement of the Ammonia Tropospheric Profile and of the <sup>15</sup>N/<sup>14</sup>N Isotopic Ratio. *Icarus* 143, 223–243. [arXiv:astro-ph/9911257](#).
- Fray, N., Bénilan, Y., Cottin, H., Gazeau, M.C., Crovisier, J., 2005. The origin of the CN radical in comets: A review from observations and models. *Planetary Space Science* 53, 1243–1262.
- Gerin, M., Marcelino, N., Biver, N., Roueff, E., Coudert, L.H., Elkeurti, M., Lis, D.C., Bockelée-

- Morvan, D., 2009. Detection of  $^{15}\text{NH}_2\text{D}$  in dense cores: a new tool for measuring the  $^{14}\text{N}/^{15}\text{N}$  ratio in the cold ISM. *A&A* 498, L9–L12. 0903.3155.
- Gilmour, I., 2003. Structural and Isotopic Analysis of Organic Matter in Carbonaceous Chondrites. *Treatise on Geochemistry* 1, 269–290.
- Hashizume, K., Chaussidon, M., Marty, B., Robert, F., 2000. Solar Wind Record on the Moon: Deciphering Presolar from Planetary Nitrogen. *Science* 290, 1142–1145.
- Hily-Blant, P., Walmsley, M., Pineau des Forêts, G., Flower, D., 2008. CN in prestellar cores. *A&A* 480, L5–L8. [arXiv:0801.2876](#).
- Hily-Blant, P., Walmsley, M., Pineau des Forêts, G., Flower, D., 2010. Nitrogen chemistry and depletion in starless cores. *A&A* 513, A41+. 1001.3930.
- Huss, G.R., Meshik, A.P., Smith, J.B., Hohenberg, C.M., 2003. Presolar diamond, silicon carbide, and graphite in carbonaceous chondrites: implications for thermal processing in the solar nebula. *Geochim. Cosmochim. Ac.* 67, 4823–4848.
- Ikeda, M., Hirota, T., Yamamoto, S., 2002. The  $\text{H}^{13}\text{CN}/\text{HC}^{15}\text{N}$  Abundance Ratio in Dense Cores: Possible Source-to-Source Variation of Isotope Abundances? *ApJ* 575, 250–256.
- Irvine, W.M., Schloerb, F.P., Crovisier, J., Fegley, Jr., B., Mumma, M.J., 2000. Comets: a Link Between Interstellar and Nebular Chemistry. *Protostars and Planets IV*, 1159.
- Jehin, E., Manfroid, J., Hutsemékers, D., Arpigny, C., Zucconi, J.M., 2009. Isotopic Ratios in Comets: Status and Perspectives. *Earth Moon and Planets* 105, 167–180.
- Kung, C.C., Clayton, R.N., 1978. Nitrogen abundances and isotopic compositions in stony meteorites. *Earth and Planetary Science Letters* 38, 421–435.
- Lis, D.C., Wootten, A., Gerin, M., Roueff, E., 2010. Nitrogen Isotopic Fractionation in Interstellar Ammonia. *ApJ* 710, L49–L52. 1001.0744.
- Lyons, J.R., Bergin, E.A., Ciesla, F.J., Davis, A.M., Desch, S.J., Hashizume, K., Lee, J.E., 2009. Timescales for the evolution of oxygen isotope compositions in the solar nebula. *Geochimica et Cosmochimica Acta* 73, 4998–5017.
- Manfroid, J., Jehin, E., Hutsemékers, D., Cochran, A., Zucconi, J.M., Arpigny, C., Schulz, R., Stüwe, J.A., Ilyin, I., 2009. The CN isotopic ratios in comets. *A&A* 503, 613–624. 0907.0311.
- Marty, B., Chaussidon, M., Wiens, R.C., Jurewicz, A.J.G., Burnett, D.S., 2011. A  $^{15}\text{N}$ -Poor Isotopic Composition for the Solar System As Shown by Genesis Solar Wind Samples. *Science* 332, 1533–.
- Marty, B., Zimmermann, L., Burnard, P.G., Wieler, R., Heber, V.S., Burnett, D.L., Wiens, R.C., Bochsler, P., 2010. Nitrogen isotopes in the recent solar wind from the analysis of Genesis targets: Evidence for large scale isotope heterogeneity in the early solar system. *Geochim. Cosmochim. Ac.* 74, 340–355.
- Meibom, A., Krot, A.N., Robert, F., Mostefaoui, S., Russell, S.S., Petaev, M.I., Gounelle, M., 2007. Nitrogen and Carbon Isotopic Composition of the Sun Inferred from a High-Temperature Solar Nebular Condensate. *ApJ* 656, L33–L36.
- Messenger, S., 2000. Identification of molecular-cloud material in interplanetary dust particles. *Nature* 404, 968–971.
- Milam, S.N., Charnley, S.B., 2012. Observations of Nitrogen Fractionation in Prestellar Cores: Nitriles Tracing Interstellar Chemistry, in: *Lunar and Planetary Institute Science Conference Abstracts*, p. 2618.
- Milam, S.N., Savage, C., Brewster, M.A., Ziurys, L.M., Wyckoff, S., 2005. The  $^{12}\text{C}/^{13}\text{C}$  Isotope Gradient Derived from Millimeter Transitions of CN: The Case for Galactic Chemical Evolution. *ApJ* 634, 1126–1132.
- Okumura, F., Mimura, K., 2011. Gradual and stepwise pyrolyses of insoluble organic matter from the Murchison meteorite revealing chemical structure and isotopic distribution. *Geochim. Cosmochim. Ac.* 75, 7063–7080.
- Owen, T., Mahaffy, P.R., Niemann, H.B., Atreya, S., Wong, M., 2001. Protosolar Nitrogen. *ApJ* 553, L77–L79.
- Padovani, M., Walmsley, C.M., Tafalla, M., Hily-Blant, P., Pineau des Forêts, G., 2011. Hydrogen cyanide and isocyanide in prestellar cores. *A&A* 534, A77.
- Paganini, L., Villanueva, G.L., Lara, L.M., Lin, Z.Y., Küppers, M., Hartogh, P., Faure, A., 2010. HCN Spectroscopy of Comet 73P/Schwassmann-Wachmann 3. A Study of Gas Evolution and its Link to CN. *ApJ* 715, 1258–1269.
- Pizzarello, S., Feng, X., Epstein, S., Cronin, J.R., 1994. Isotopic analyses of nitrogenous compounds from the Murchison meteorite: ammonia, amines, amino acids, and polar hydrocar-

- bons. *Geochim. Cosmochim. Ac.* 58, 5579–5587.
- Ratajczak, A., Quirico, E., Faure, A., Schmitt, B., Ceccarelli, C., 2009. Hydrogen/deuterium exchange in interstellar ice analogs. *A&A* 496, L21–L24.
- Remusat, L., Derenne, S., Robert, F., Knicker, H., 2005. New pyrolytic and spectroscopic data on Orgueil and Murchison insoluble organic matter: A different origin than soluble? *Geochim. Cosmochim. Ac.* 69, 3919–3932.
- Rodgers, S.D., Charnley, S.B., 2008. Nitrogen Isotopic Fractionation of Interstellar Nitriles. *ApJ* 689, 1448–1455.
- Roueff, E., Lis, D.C., van der Tak, F.F.S., Gerin, M., Goldsmith, P.F., 2005. Interstellar deuterated ammonia: from  $\text{NH}_3$  to  $\text{ND}_3$ . *A&A* 438, 585–598. [arXiv:astro-ph/0504445](#).
- Schmitt-Koplin, P., Gabelica, Z., Gougeon, R.D., Fekete, A., Kanawatu, B., Harir, M., Gebefuegi, I., Eckel, G., Hertkorn, N., 2010. High molecular diversity of extraterrestrial organic matter in murchison meteorite revealed 40 years after its fall. *PNAS* 107, 2763–2768.
- Sephton, M.A., Verchovsky, A.B., Bland, P.A., Gilmour, I., Grady, M.M., Wright, I.P., 2003. Investigating the variations in carbon and nitrogen isotopes in carbonaceous chondrites. *Geochim. Cosmochim. Ac.* 67, 2093–2108.
- Sephton, M.A., Wright, I.P., Gilmour, I., de Leeuw, J.W., Grady, M.M., Pillinger, C.T., 2002. High molecular weight organic matter in martian meteorites. *Planetary Space Science* 50, 711–716.
- Terzieva, R., Herbst, E., 2000. The possibility of nitrogen isotopic fractionation in interstellar clouds. *MNRAS* 317, 563–568.
- van der Tak, F.F.S., Black, J.H., Schöier, F.L., Jansen, D.J., van Dishoeck, E.F., 2007. A computer program for fast non-LTE analysis of interstellar line spectra. With diagnostic plots to interpret observed line intensity ratios. *A&A* 468, 627–635.
- Wirström, E.S., Charnley, S.B., Cordiner, M.A., Milam, S.N., 2012. Isotopic Anomalies in Primitive Solar System Matter: Spin-state-dependent Fractionation of Nitrogen and Deuterium in Interstellar Clouds. *ApJ* 757, L11. 1208.0192.